Mechanics and Mechanical Engineering
Vol. 12, No. 1 (2008) 51–60

Kinetics of the Inspection Robot

Józef Giergiel and Krzysztof Kurc
Department of Applied Mechanics and Robotics, Rzeszow University of Technology

Received (1 October 2007)
Revised (15 November 2007)
Accepted (8 January 2008)

Were presented in the article modelling by the description kinematics and of dynamics of the own design of the inspective robot, to permit monitoring and the analysis of the technical state of internal parts of pipelines. After modelling the kinetics they made an analysis utilizing symbolic and numeric transformations packages of MAPLE, MATLAB/SIMULINK. An obtained graph was compared and they drew conclusions.

Keywords: kinematics, dynamics, simulations

1. Introduction

After the stage of modeling kinematics and dynamics of inverse [1, 2] a stage was carried out of modeling kinematics and dynamics of simple of inspection robot designed for inspection inside tubular pipelines about the circular section.

In case of the analysis of the simple task of dynamics it is necessary to determine parameters tied with the movement of the robot being under working of force and driving moments. Dynamic properties of the robot are expressed as changes of the position in the time depending on of force and driving moments [6, 7, 8, 9]. Solution to the simple task kinematyki is letting determine the trajectory of the point of the robot (comparing her to the given trajectory) knowing parameters tied with the movement of the robot.

2. Modeling of simple dynamics

Analysing dynamics of the inspection robot Fig. 1a [6], a replacement model of the robot was accepted Fig. 1b, where: 1, 6, 7 they are representing leading wheels, 2 wheel arms, motor, camera and strengthening sheet metal, 3 left part of the Cardan joint with cogwheel, 4 right part of the Cardan joint with arms of driving wheels, 5 driving wheels (rotor). Marked angular velocity it:

$\dot{\alpha}$ – angular velocity on the shaft of the motor,

$\dot{\alpha}_1$ – angular velocity leading wheel,

$\dot{\alpha}_L$ – angular velocity of left part of the Cardan joint,
$\dot{\alpha}_P$ –angular velocity of right part of the Cardan joint,
$\dot{\alpha}_5$ – angular velocity driving wheel.

The movement of the model was characterized using equations Lagrange'a II of kind (1)

$$\frac{d}{dt}\left(\frac{\partial E}{\partial \dot{q}_j}\right) - \left(\frac{\partial E}{\partial q_j}\right) = Q_j. \tag{1}$$

Kinetic energy of the setup is an amount of energy of kinetic each components:

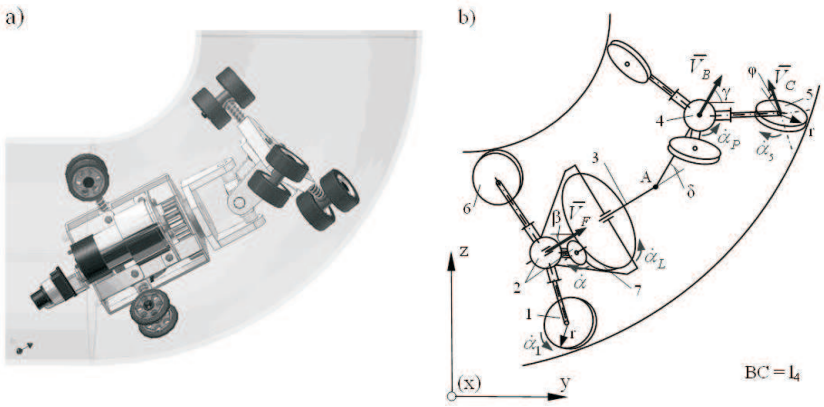

Figure 1 a) Inspection robot, b) Model of the robot

$$E = E_1 + E_2 + E_3 + E_4 + E_5 + E_6 + E_7, \tag{2}$$

where:

$$E_1 = \frac{1}{2}m_1\left(V_F + \dot{\beta}l_4\right)^2 + \frac{1}{2}I_{Gx}\dot{\alpha}_1^2 \quad \text{– leading wheel 1} \tag{3}$$

$$E_2 = \frac{1}{2}m_1\left(V_F - \dot{\beta}l_4\sin\psi\right)^2 + \frac{1}{2}I_{Hx}\dot{\alpha}_1^2 \quad \text{– leading wheel 6} \tag{4}$$

$$E_3 = \frac{1}{2}m_1\left(V_F - \dot{\beta}l_4\sin\psi\right)^2 + \frac{1}{2}I_{Kx}\dot{\alpha}_1^2 \quad \text{– leading wheel 7} \tag{5}$$

$$E_4 = \frac{1}{2}m_2V_F^2 + \frac{1}{2}I_{Fx}\dot{\beta}^2 \quad \text{– frame of the robot} \tag{6}$$

$$E_5 = \frac{1}{2}m_3V_F^2 + \frac{1}{2}I_{Fy}\dot{\alpha}_L^2 + \frac{1}{2}I_{Fx}\dot{\beta}^2 \quad \text{– left part of the Cardan joint} \tag{7}$$

$$E_6 = \frac{1}{2}m_4V_B^2 + \frac{1}{2}I_{By}\dot{\alpha}_P^2 + \frac{1}{2}I_{Bx}\dot{\gamma}^2 \quad \text{– right part of the Cardan joint} \tag{8}$$

$$E_7 = 3\left(\frac{1}{2}m_5V_C^2 + \frac{1}{2}I_{Cy}\dot{\alpha}_5^2 + \frac{1}{2}I_{Cx}\dot{\gamma}^2\right) \quad \text{– driving wheels} \tag{9}$$

Visible in dependence corner ψ were presented on Fig 2.

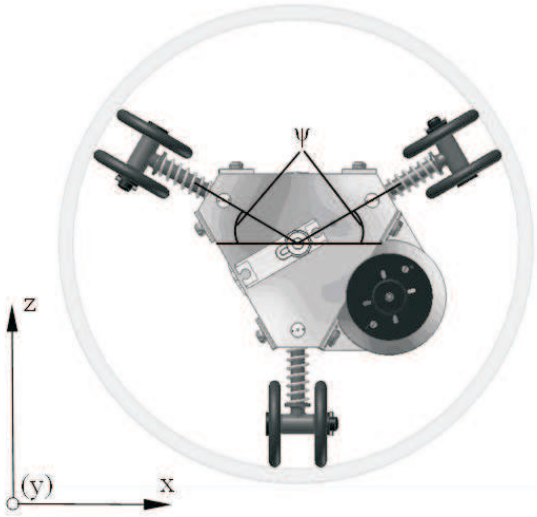

Figure 2 Marked corner ψ

Generalized force appointed from dependence:

$$Q\delta\alpha = \delta L, \tag{10}$$

where:

$\delta\alpha$ – virtual circulation on the shaft of the motor

δL – virtual work:

$$\delta L = \delta L^{(1)} + \delta L^{(2)} + \delta L^{(3)} + \delta L^{(4)} + \delta L^{(5)} + \delta L^{(6)} + \delta L^{(7)}. \tag{11}$$

Virtual work executed by members of the robot during transport Fig. 3. it:

$$\begin{aligned}
\delta L^{(1)} &= (-N_1 f_1 - G_1 r \sin\beta)\,\delta\alpha_1 && (12)\\
\delta L^{(2)} &= (-N_1 f_1 - G_1 r \sin\beta)\,\delta\alpha_1 && (13)\\
\delta L^{(3)} &= (-N_1 f_1 - G_1 r \sin\beta)\,\delta\alpha_1 && (14)\\
\delta L^{(4)} &= -G_2 \sin\beta \delta r_F && (15)\\
\delta L^{(5)} &= -G_3 \sin\beta \delta r_F && (16)\\
\delta L^{(6)} &= -G_4 \sin\gamma \delta r_B && (17)\\
\delta L^{(7)} &= (-3N_2 f_2 - 3G_5 r \sin\gamma + \mathrm{Pr})\,\delta\alpha_5 && (18)
\end{aligned}$$

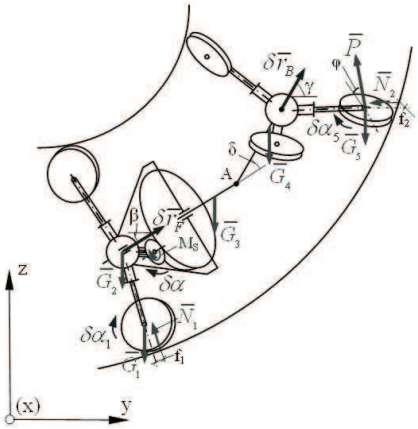

Figure 3 Model of the robot along with put strength

Introducing dependence kinematics and executing necessary mathematical operations to Maple resulting from equalization Lagrange'a, interesting us the angle acceleration of the motor has the form during transport of the robot:

$$\ddot{\alpha} = \frac{z_k \pi r \cos\delta}{{z_s}^2} \frac{A_0 + (A_1 \cos\delta - 60 r G_4 z_s \sin\gamma\,(l_4 + r))\tan\varphi}{A_2 + (A_3 \cos\delta^2 + A_4)\tan\varphi^2} \tag{19}$$

where

$$\begin{aligned}
A_0 &= \pi\left(M_s z_k r \cos\varphi^2 + (-3N_2 f_2 z_s l_4 - 3rG_5 \sin\gamma z_s l_4)\cos\varphi\right)\\
A_1 &= -180 z_s N_1 f_1\,(l_4 + r) - 60 m_1 l_4 z_s \ddot{\beta} r\,(l_4 + r)\\
&\quad -60 r z_s \sin\beta\,(3l_4 G_1 + 3rG_1 + G_3 l_4 + rG_3 + G_2 l_4 + rG_2)\\
&\quad +120 m_1 l_4 z_s \ddot{\beta} r \sin\psi\,(l_4 + r)\\
A_2 &= \pi^2\left(r^2 I_{Fy}\cos\delta^2 + r^2 I_{By} + \left(3l_4^2 m_5 r^2 + 3l_4^2 I_{Cy}\right)\cos\varphi^2\right)\\
A_3 &= 7200 r^3 l_4 m_3 + 3600 r^2 l_4^2 m_3 + 10800 I_{Gx} l_4^2 + 21600 I_{Gx} l_4 r\\
&\quad +3600 r^2 l_4^2 m_2 + 21600 r^3 l_4 m_1 + 7200 r^3 l_4 m_2 + 3600 r^4 m_3\\
&\quad +10800 I_{Gx} r^2 + 10800 r^4 m_1 + 3600 r^4 m_2 + 10800 r^2 l_4^2 m_1\\
A_4 &= 7200 m_4 r^3 l_4 + 3600 m_4 r^4 + 3600 m_4 r^2 l_4^2
\end{aligned}$$

Dependence (19) were taken advantage to the simulation of the simple task of dynamics calculated angle of rotation, angular velocity and angular acceleration on the shaft of the motor.

2.1. *Simulations of simple dynamics*

A conducted computer simulation remained on the basis of the above-mentioned description in the package MATLAB/SIMULINK. Visible in equalization coefficients determining geometry masses, mass moments of inertia, radius, distances, angles, force pressure, arms of resistance rolling were read from physical parame-

ters software CAD [3,4,5], whom a robot was designed Fig. 1a, or were appointed experimentally. Constant coefficients it:

$m_1 = 0,012$ kg; $I_{Gx} = 0,000000599$ kgm^2;
$m_2 = 0,328$ kg; $f_1 = 0,0015$ m;
$m_3 = 0,075$ kg; $f_2 = 0,003$ m;
$m_4 = 0,05$ kg; $N_1 = 4,4$ N;
$m_5 = 0,045$ kg; $N_2 = 6,1$ N;
$I_{By} = 0,000020269$ kgm^2; $l_4 = 0,057$;
$I_{Bz} = 0,000034692$ kgm^2; $r = 0,015$;
$I_{Cy} = 0,000002955$ kgm^2; $z_s = 12$;
$I_{Cz} = 0,000001971$ kgm^2; $z_k = 48$;
$I_{Fy} = 0,000071239$ kgm^2; $\phi = \pi/18$;
$I_{Fz} = 0,000018807$ kgm^2; $\psi = \pi/6$.

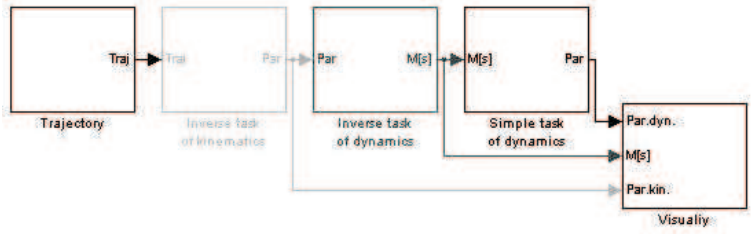

Figure 4 MATLAB/SIMULINK flowchart of the simple task of dynamics

The remaining non-linear parameters dependent on the time so like the moment on the shaft of the motor, angular acceleration of the frame whether corners in the Cardan joint were appointed in the inverse task of dynamics or they assumed making them dependent on the profile of the tested pipe in the block trajectory Fig. 4. For example from the inverse task of dynamics for the assumed trajectory of the B point of the robot (simple horizontal – curve – simple vertical) Fig. 5. were received moment on the shaft of the motor Fig. 6.

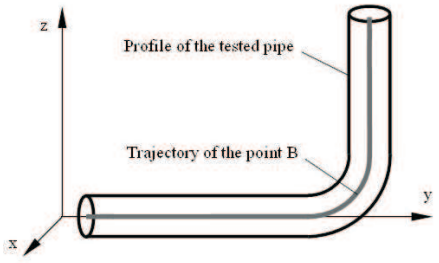

Figure 5 Assumed trajectory of the B point of the robot

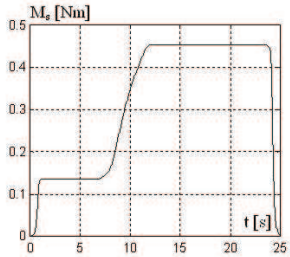

Figure 6 Driving moment of the motor

Were determined from the simple task of dynamics angle of rotation, angular velocity and angular acceleration on the shaft of the motor. Appointed parameters

were compared obtained out of the inverse task with parameters kinematics Fig. 4. and a difference of errors was shown.

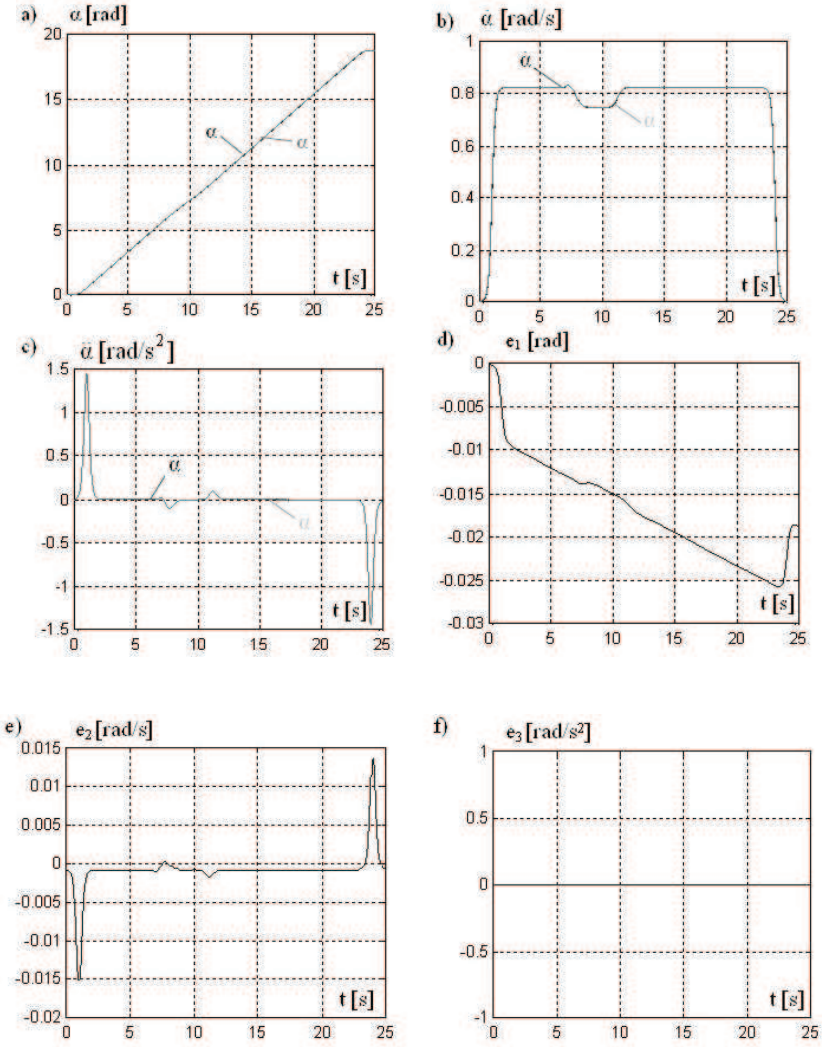

Figure 7 a), b), c) Temporary course angle of rotation, angular velocity and angular acceleration from the inverse task kinematics in comparing to course from the simple task dynamics. d), e), f) Difference of errors between this course

Error e_1 were defined as difference angles of rotation, error e_2 as difference angular velocity however error e_3 as difference angular acceleration on the shaft of the motor from the simple task of dynamics and from the inverse task kinematics. Comparing these errors it is possible to observe Fig. 7.d, e, f, an error is biggest from errors e_1

however smallest equal to zero error e_3. These errors are resulting from the quantity to a large degree integral and of differentiations of signals during the process of the simulation.

The analysis carried out and the simulation of the task of simple dynamics she will be utilized in the more far-away stage during the analysis and the simulation in the task simple kinematics. The analysis of the simple task of dynamics will serve in the future to identification of the model of the inspection robot.

3. Modeling of simple kinematics

Solution to the simple task kinematics he will permit correctness of executed counts to check. This check will consist e.g. on assigning the robot to the trajectory and for comparing of her to the given trajectory. The specification of the trajectory will be tied with the transformation of equalization and performing in them variable parameters they will remain "taken" from the simple task of dynamics. Task simple of kinematics would be able to be realized after the inverse task of kinematics but realization after both tasks of dynamics he is checking transformations and counts of the inverse task kinematics and both of tasks of dynamics.

During modelling of inverse kinematics [1] one of dependence was output:

$$\frac{V_B \pi}{60\,(l_4 + r_2)\,tg\varphi} = \frac{z_S \dot{\alpha}}{z_K \cos\delta}. \tag{20}$$

In order to determine the corner in the Cardan joint δ equation (20) were transformed to following forms:

$$\delta = \arccos\left(\frac{z_S \dot{\alpha} 60\,(l_4 + r_2)\,tg\varphi}{V_B \pi z_K}\right). \tag{21}$$

In equation (21) angular velocity $\dot{\alpha}$ she is being taken from the simple task of dynamics. Determining $\dot{\delta}$ were calculated angular velocity of the rotor during transport through the curved section of the pipe (trajectory):

$$\dot{\gamma} = \dot{\beta} + \dot{\delta}. \tag{22}$$

Integrating $\dot{\gamma}$ were received angle of rotation of the rotor γ, were taken advantage for assigning the B point of the robot to the trajectory.

$$y_B = y_A + l_1 \cos\gamma. \tag{23}$$

$$z_B = z_A + l_1 \sin\gamma. \tag{24}$$

The received trajectory was compared to the trajectory given during the simulation.

3.1. *Simulations of simple kinematics*

On the basis of the above-mentioned description were taken computer simulation in the package MATLAB/SIMULINK according to the block diagram Fig. 8.

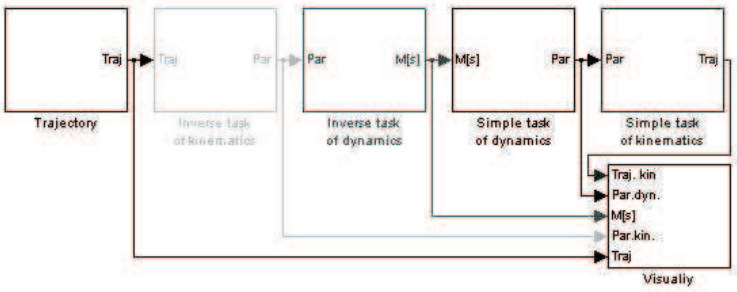

Figure 8 MATLAB/SIMULINK flowchart of the simple task kinematics

In the block ,,visually" Fig. 8. the was compared trajectory of the point B appointed from the simple task of dynamics with the given trajectory. Components of the given and received trajectory from the simple task kinematics of point B of the robot were presented in the function of the time Fig. 9.a, b and difference of errors between component Fig. 9.c, d.

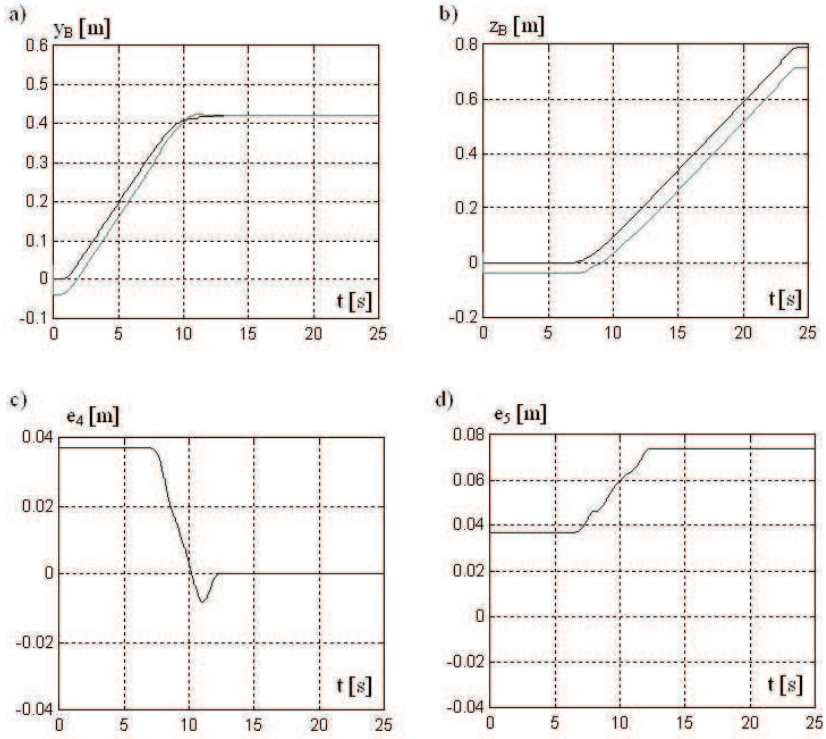

Figure 9 a, b) Components of the trajectory of the B point of the robot in the function of the time. c, d) Differences of errors between component

Error e_4 it is difference between the given component and received component y_B of the robot, however e_5 between the given component and received component z_B of the robot. On Fig.10 a component was presented y_B in the function z_B.

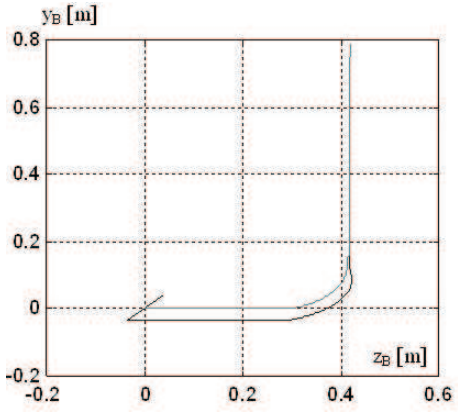

Figure 10 Given and received trajectory of the B point of the robot

Conspicuous errors are resulting from the numeric differentiation and integration. Initiated in the first step of counts they are vanishing Fig. 9.c, what is tied with the specificity of course Fig. 9.a or is maintaining himself until the end of the time of the simulation Fig. 9.d. Of error so it was possible to expect in the time already of determining of angle velocity on the shaft of the motor from the simple task of dynamics and comparisons her at the angle velocity from the inverse task kinematics Fig. 7.b. Error received already then e_2 Fig. 7.e he was signalling about the difference between trajectories, because angle velocity on the shaft of the engine from the simple task of dynamics she was supposed to remain utilized in more far-away counts of equalization of the simple task kinematics, how it happened also.

4. Summary

In methodology of the description of the movement of the inspection robot symbolic and numeric transformations were utilized for the package Maple, Matlab/Simulink, it is possible to apply for analysis kinematics and of dynamics of mobile robots, moving after various trajectories of the movement.

The analysis of dynamics of mobile robots is being carried out in order solving of the problem of control system of the movement of this type. Having inspection of pipes executed from the various kind of materials on the remark the implemented control of the robot will be happening behind help of radio or wire broadcast.

Determined parameters during the analysis kinematics and of dynamice they will also be utilized in the comparative purpose obtained with parameters which will remain from the simulation carried out dynamic in software of the CAE type utilizing the model of the designed robot.

She will be realized by the estimation of parameters at more far-away work and identification of the model of the mathematical real inspection robot, utilizing sensors and meter circuit.

References

[1] **Giergiel J., Kurc K, Żylski W.**: Modeling of kinematics of the inspective robot, X International Seminar of Applied Mechanics, Politechnika lska, Wisa 2006, ISBN 83-60102-30-9.

[2] **Giergiel J., Kurc K.**: Modeling of dynamics of the inspective robot, X International Seminar of Applied Mechanics, Politechnika lska, Wisa 2006, ISBN 83-60102-30-9.

[3] **Giergiel J., Kurc K.**: Construction, analysis and simulation of the inspective robot, XI International Conference Computer Simulation in Machine Design – Cosim 2006, Politechnika Warszawska, Krynica Zdrój 2006, ISBN 83-89703-12-2.

[4] **Giergiel J., Kurc K.**: Mechatronics of the inspective robot, *Mechanics and Mechanical Engineering*, Vol. 10, No. 1, 2006, Technical University of Lodz.

[5] **Giergiel J., Kurc K.**: Robot inspekcyjny do przewodów rurowych, PAK nr. **11**, Warszawa 2004.

[6] **Giergiel J., Buratowski T., Kurc K.**: Podstawy robotyki i mechatroniki. Cz 1 Wprowadzenie do robotyki, Wydawnictwo KRiDM AGH, Kraków 2004.

[7] **Giergiel J., Hendzel Z., Żylski W.**: Kinematyka, dynamika i sterowanie mobilnych robotów koowych w ujciu mechatronicznym, Monografie, Wydz.IMiR, AGH Kraków, 2000.

[8] **Craig J. J.**: Wprowadzenie do robotyki, WNT, Warszawa, 1993.

[9] **Spong M. W., Vidyasagar M.**:Dynamika i sterowanie robotów, WNT, Warszawa, 1997.

The work is a part of the research project No. N N501 0108 33